Investigation of the combined effect of air pockets and air bubbles on fluid transients

Oscar Pozos-Estrada

ABSTRACT

This paper presents numerical and experimental investigations of the combined effect on pressure transients of air pockets and homogenous water–air bubble mixtures. An air pocket can accumulate at a high point of a pipeline along the control section located at the transition between pipes with sub- and supercritical slope, forcing open channel flow conditions underneath the pocket that ends in a hydraulic jump at the downward sloping pipe. The turbulence action at the jump generates small air bubbles that are entrained and transported along the pipe producing a two-component bubbly flow within the continuous liquid phase. A numerical model is developed, combining the explicit–implicit scheme proposed by McGuire and Morris and the method of characteristics for solving the quasi-linear hyperbolic partial differential equations for transient two-phase flow expressed in conservation form. To verify the proposed model, an experimental apparatus made of PVC was used to carry out hydraulic transient experiments. Tests were conducted in a tank–pipe–valve system and a valve with a pneumatic actuator at the downstream end generated transients. Numerical results at the test section pipe compares favorably with experimental data. The results show that pressure transients are significantly reduced with increasing air-pocket volumes and bubbly flow air content.

Key words | air bubble, air pocket, hydraulic jump, hydraulic transient flow, water–air mixture

Oscar Pozos-Estrada
Instituto de Ingeniería, Department of Hydraulic Engineering,
Universidad Nacional Autónoma de México,
Cd. Universitaria, Mexico City C.P. 04510,
Mexico
E-mail: *opozose@iingen.unam.mx*

INTRODUCTION

Air in pipelines cannot be always completely eliminated but understanding the ways how it enters a pipe helps engineers to minimize its occurrence. Air in the line comes from different sources, for instance, a pipeline is full of air during its filling. If the air is not completely released through air valves, vents, and standpipes, air may remain at high points throughout the system in the form of air pockets (Falvey 1980). Air also enters through pumps; they introduce air by the vortex action of the suction in quantities of 5% to 10% of the water discharge (Qiu 1995). When pressure in a pipeline decreases below the atmospheric pressure, air can enter by means of damaged packing at joints and valves (Wisner *et al.* 1975). Moreover, water at standard temperature and pressure can contain at least 2% of dissolved air by volume (Fox 1977).

Entrapped air in pipelines may lead to a variety of problems. For instance, air pockets accumulated at summits of closed conduits can throttle the flow, which generates an increment of head losses (Richards 1962; Edmunds 1979). Incorrect readings on measurement devices are produced by free air. Vibrations are caused by the transition from a partly full pipe to a full pipe because of the presence of air pockets. Important quantities of accumulated air cause blowbacks that drive to vibrations and structural damage (Sailer 1955). Air may build up in important quantities such that the air pockets can cause the partial or complete blockage of flowing water, reducing the capacity of the pumping systems as well as the gravity pipeline systems (Thomas 2003). Blockage distributed along a pipeline diminishes its capacity and meanwhile increases energy costs (Sun *et al.* 2016).

doi: 10.2166/hydro.2017.018

If the entrained air is transported along a pipeline by the flowing water, it may accumulate in the form of air pockets at its summits formed by the change in pipe slope, when air valves are not installed. Although air valves are placed, they might fail and air will not be released. Various researchers have studied stationary air pockets at summits of pipelines that force water under the pockets to achieve free surface flow conditions (Walski *et al.* 1994; Pozos 2007; Pozos *et al.* 2010).

In the same way, the large pressure peaks originated immediately after an air pocket has been released through an air/vacuum valve or through an orifice, during the rapid filling of a pipeline have been investigated experimentally and theoretically by several researchers. Some of them have studied the air release through an air valve located at a high point of an undulating pipeline (Izquierdo *et al.* 1999; Arregui *et al.* 2003; Kruinsbrick *et al.* 2004; Carlos *et al.* 2011; Balacco *et al.* 2015; Apollonio *et al.* 2016), while others considered an orifice at the end of a horizontal pipe (Zhou *et al.* 2002; Lee 2005). The general findings of the above authors were focused on the factors affecting the peak transient pressure, for instance, the size of the orifices, the location and length of the entrapped air pocket, the driving pressure head, and the water column length. Recently, Zhou *et al.* (2013) investigated numerically and experimentally the transient pressure associated with rapid filling of an undulating pipeline containing two entrapped air pockets. It is important to highlight that during the study air release was not considered. The authors found that when the two air pockets in length are very different, the maximum increment of the pressure always occurs in the smaller air pocket, irrespective of the length of the blocking column. Likewise, the case when the two entrapped pockets have a similar length is the most complicated and dangerous, since they can generate an extreme pressure surge.

In a similar manner, two-phase flow with air pockets is present in pipes of storm-water and sewer systems, causing many unpleasant situations and accidents because of rapid water filling due to an extreme storm, above the designed values of the systems. High-pressure variation provoked by the appearance and releasing of air pockets has caused significant damage in pipes, for example, the incidents in the city of Edmonton, Alberta, Canada (Zhou *et al.* 2002) and Minneapolis, Minnesota, USA (Wright *et al.* 2011).

Many numerical models have been implemented to investigate transient changes in the flow rate and pressure for the simultaneous occurrence of free surface and pressurized flows in sewer systems. Most recent models are based on the Saint Venant equations and the concept of the Preissmann Slot (Vasconcelos 2005; Leon 2006). More recently, Leon *et al.* (2010), Trindade & Vasconcelos (2013), and Vasconcelos *et al.* (2015) have developed more sophisticated numerical models to simulate entrapment and release of air pockets during rapid filling of large stormwater systems.

Regarding fluid transients the effect of entrained air in water pipeline systems may be either beneficial or harmful; it dependents on the volume of air, its distribution and location, the characteristics of the pipeline profile, as well as the causes of the transient (Martin 1976, 1996). In water and wastewater pipelines, usually entrapped air present is present either as stationary pockets or as small air bubbles dispersed within the continuous liquid phase (Lauchlan *et al.* 2005). The consequences related to entrapped or entrained air on fluid transients are considered in the following sequence.

Gahan (2004) highlighted that small and large stationary air pockets located at high points of pipelines can be defined in terms of their effect on hydraulic transients, but there are limits to the volumes of air, outside of which, these effects do not occur. Several researchers have shown that peak pressure transients can be enhanced by small air pockets, since they can act as unwanted nonlinear springs that amplify surge pressures, sufficient to cause pipe failure (Jönsson 1985, 1992; Burrows & Qiu 1995; Qiu & Burrows 1996; Izquierdo *et al.* 1999; Burrows 2003; Pozos-Estrada *et al.* 2012, 2016; Martins *et al.* 2015; Besharat *et al.* 2016).

On the other hand, when the volume of air that remains localized at a high point is large this usually behaves as an air cushion that absorbs the transient pressure waves (Thorley 2004). Stephenson (1997) stated that the formation of large air pockets in pipelines, if adequately managed, may be beneficially used to reduce water hammer.

Likewise, in transient flow, air bubbles distributed within the continuous liquid phase may arise due to free air or as a result of the release of dissolved air in water, when the pressure drops or temperature increases above its saturation level. Liquid–gas mixture flows are complicated by a number of factors. First, the internal structure

adopted by the multiplicity of liquid–gas interfaces become very complicated in physical form. Second, the mixture has relatively high density due to its liquid component and has a low bulk modulus due to the gas component. The mixtures have low propagation velocities for pressure disturbances (Davis 1980). The dampening of the pressure waves has an overall beneficial effect on pipeline systems. Ewing (1980) stated that the damping occurs due to dispersion breaking down of the main wave surge into shorter wave length components, which are damped out more readily. Pearsall (1965) found that air dispersed in water as small bubbles results in an important reduction of the pressure surges, the most likely cause of the damping observed is due to the internal reflection of the acoustic wave in bubbly water.

Based on the above, it can be stated that several authors have reported the effects of trapped air on hydraulic transients in pipeline systems. However, usually these studies considered a single horizontal pipe, whereas most of the pipelines for water supply and the transport of wastewater are formed of upward and downward sloping pipes. Likewise, researchers that have investigated pressure transients with entrapped pockets in undulating pipelines have not considered the two-phase bubbly air–water mixtures that commonly occur downstream of the air pockets ending with a hydraulic jump. This prompted the author to study numerically and experimentally the combined effects of both air pockets and homogenous water–air mixtures on hydraulic transients.

In this paper, a numerical model based on an explicit–implicit scheme proposed by McGuire & Morris (1975) and the method of characteristics (MOC) was developed to simulate fluid transients with stationary air pockets ending in a hydraulic jump that entrain small air bubbles producing a two-component bubbly flow within the continuous liquid phase. To verify the proposed model, an experimental apparatus was designed and constructed; the setup has a test section that simulates a high point of a pipeline with an undulating profile. In the experiments, the hydraulic transients were generated by the sudden closure of a butterfly valve with double acting pneumatic actuator located at the downstream end of the test section. It was found that the numerical and experimental results were in good agreement. Further, the results showed that pressure transients were significantly reduced with increasing air-pocket volumes and bubbly flow air content.

NUMERICAL MODEL

The numerical model was developed with the main goal to investigate the combined effect of both air pockets and water–air mixtures on hydraulic transients. The numerical simulation of fluid transients taking into account stationary air pockets accumulated at summits of a pipeline system and a bubbly flow at the downstream end of them is evaluated by using the homogeneous model. The procedure to solve the equations used in the analytical model is the explicit–implicit method proposed by McGuire & Morris (1975) and the MOC.

The effect of the air pockets is taken into account as outlined below. Some assumptions made by Burrows & Qiu (1995) are as follows. (a) The MOC is used to obtain the ordinary differential equations. They are then solved along characteristic lines with first-order approximation and without interpolation to eliminate numerical instability. Numerical models based on the MOC are known to give accurate results and have been demonstrated to be effective (Almeida & Ramos 2010). They have been successfully applied in the design and analysis of water pipe systems involving transient cavitation, air pockets, and leak detection (Burrows & Qiu 1995; Ivetic 2004; Soares *et al.* 2011). (b) Known air-pocket volumes can be placed at selected nodal points; it is assumed that the pocket included will not result in water column separation all along the numerical simulations. In addition, the air pocket does not occupy the entire cross-section of the conduit and remains in its original position during the time scale of the hydraulic transient. (c) The air in the pocket is supposed to follow the polytropic equation of state. (d) Friction and local losses are considered in the analytical model. (e) For simulations, the known air-pocket volumes are located at a junction between adjacent pipe reaches. It is important to emphasize that there are situations when it is quite permissible to use a lumped parameter analysis of portions of piping systems (Wylie *et al.* 1993). In this case the lumped elements are the air pockets that interact with a compatibility equation (Equation (1)) in the pipeline. During the investigation air

pockets were considered as accumulators, where the pressure at any instant is the same throughout the air volume. The compressibility of the liquid in the accumulator can be neglected since it is very small compared with the air compressibility.

Figure 1 shows a stationary air pocket located at the *i*th junction of a pipeline followed by a hydraulic jump, indicating the hydraulic grade line with and without an air pocket. It is apparent that in the case of the presence of an air pocket, the total head loss across the pipeline section is caused by pipe friction and local losses, as well as the head loss as a result of the presence of the air pocket and the hydraulic jump generated turbulence.

The air pocket polytropic change given by Equation (1) is used as boundary condition:

$$H_A V^{\psi} = C \tag{1}$$

where H_A is the absolute head (m), V is the air-pocket volume (m^3), C is constant obtained from the initial steady-state condition for the air pocket, ψ is the polytropic exponent that ranged from 1.0 to 1.4. In this investigation, $\psi = 1.4$ was employed, since a fast transient occurred after the rapid closure of a butterfly valve. Further, various researchers have demonstrated experimentally and numerically that fast transients with entrapped air pockets are better simulated with $\psi = 1.4$ (Lee & Martin 1999; De Martino *et al.* 2000; Fuertes *et al.* 2000; Martin & Lee 2000). In addition, Zhou (2000), Lee (2005), and Zhou *et al.* (2013) showed that the peak pressure of an entrapped air pocket in a rapidly filling pipeline is better predicted with $\psi = 1.4$.

Equation (1) can be also presented as:

$$(H_{U_{i,n+1}} - z + H_b) V^{\psi}_{U_{i,n+1}} = C \tag{2}$$

where $H_{U_{i,n+1}}$ is the elevation of the hydraulic grade line at section $(i, n+1)$ at the end of the time step (m), z is the distance to the centreline of pipe above datum (m), H_b is the barometric pressure head (m), $V_{U_{i,n+1}}$ is the air-pocket volume at the end of the time step (m^3).

It is important to highlight that the subscript U refers to the variables that are unknown at the end of the time step $t + \Delta t$, and the variables without the subscript U are known at the beginning of the time step t. In the following discussion, a t denotes the beginning of the time step and $t + \Delta t$ refers to the end of the time step.

The conservation of mass equation at the air pocket can be written as:

$$V_{U_{i,n+1}} = V_i + \frac{\Delta t}{2}\left[(Q_{U_{i+1,1}} + Q_{i+1,1}) - (Q_{U_{i,n+1}} + Q_{i,n+1})\right] \tag{3}$$

where V_i is the volume of air at t, Δt is the time step (s), $Q_{i,n+1}$ and $Q_{i+1,1}$ are the water discharges at the beginning and the end of the air pocket at t, respectively. $Q_{U_{i,n+1}}$ and $Q_{U_{i+1,1}}$ are

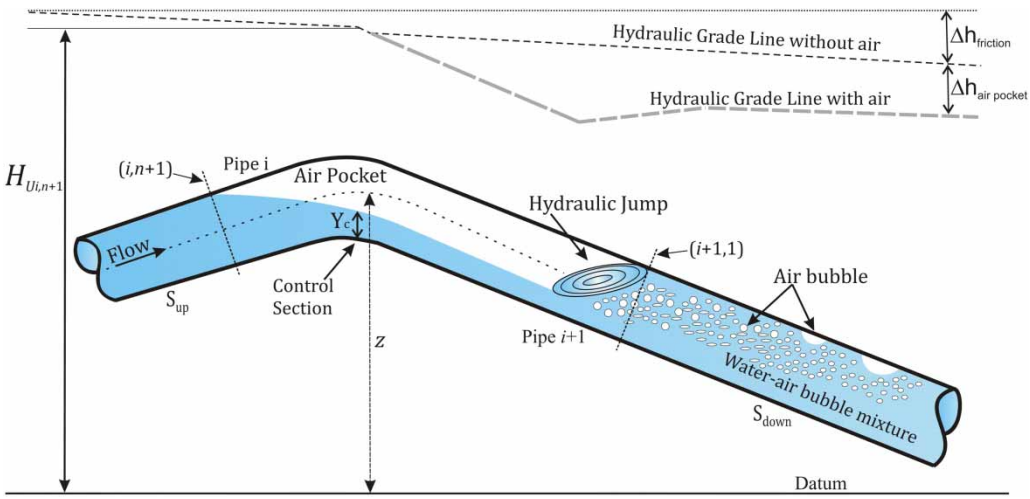

Figure 1 | Notation for the air pocket location.

the water discharges at the beginning and the end of the air pocket at $t+\Delta t$, respectively.

Since the boundary conditions are simulated by use of the MOC, then the positive and negative characteristic equations at the end of each computational time step are defined as:

$$Q_{U_{i,n+1}} = C_{(+)} - B_{c_i} H_{U_{i,n+1}} \tag{4}$$

$$Q_{U_{i+1,1}} = C_{(-)} + B_{c_{i+1}} H_{U_{i+1,1}} \tag{5}$$

Further, as can be seen from Figure 1, upstream from the air pocket the conduit flows full (no air). Likewise, downstream from the pocket the agitation present in the hydraulic jump caused the water to entrain air and mix it with the flowing water producing a two-component bubbly flow within the continuous liquid phase. For the analysis of the transients under these conditions, the effect of air-void fraction on the celerity at the downward sloping pipe should be considered. Therefore, the numerical model herein proposed evaluates the transient pressures upstream from the pocket by using the MOC including the boundaries with a celerity for water alone. On the other hand, downstream from the pocket the characteristics equations are only applied to compute the boundary conditions with a celerity for the homogenous water–air mixture, and the interior sections are simulated by means of the explicit–implicit scheme proposed by McGuire & Morris (1975) that is described in detail within this section.

Then, based on the above, the constants $C_{(+)}$, $C_{(-)}$, B_{c_i} and $B_{c_{i+1}}$ used in Equations (4) and (5) may be written as:

$$C_{(+)} = Q_{i,n+1} + B_{c_i} H_{i,n+1} - \frac{f_i \Delta t_i}{2 D_i A_{i_i}} Q_{i,n+1} \left| Q_{i,n+1} \right| \tag{6}$$

$$C_{(-)} = Q_{i+1,1} - B_{c_{i+1}} H_{i+1,1} - \frac{f_{i+1} \Delta t_{i+1}}{2 D_{i+1} A_{i+1}} Q_{i+1,1} \left| Q_{i+1,1} \right| \tag{7}$$

$$B_{c_i} = \frac{g A_i}{c_i} \tag{8}$$

$$B_{c_{i+1}} = \frac{g A_{i+1}}{c_{m_{i+1}}} \tag{9}$$

where g is the acceleration due to gravity (m/s^2), D is the internal diameter of the pipe (m), f is the Darcy–Weisbach roughness coefficient, A is the total cross section area of the pipe (m^2), c is the celerity for water alone (m/s), and c_m is the celerity for presence of the water–air mixture (m/s).

Equation (10) was used in the numerical model to evaluate c, the celerity in the presence of water only (Wylie *et al.* 1993):

$$c = \sqrt{\frac{(K_w/\rho)}{1 + (K_w/E)\,(D/e)}} \tag{10}$$

where ρ is the water density (kg/m^3), K_w is the bulk modulus of elasticity of water (Pa), E is the Young's modulus of elasticity of the pipe material (Pa), D and e are the internal diameter and the wall thickness of the pipe (m), respectively.

Furthermore, it is well known that small quantities of free air in the form of bubbles in liquids cause the celerity to be reduced substantially from that in the pure liquid itself (Kobori *et al.* 1955; Pearsall 1965; Ewing 1980). Numerous researchers have presented expressions to evaluate the wave propagation speed in the water–air mixture during the fluid transients (Kalkwijk & Kranenburg 1971; Fanelli & Reali 1975; Raiteri & Siccardi 1975; Rath 1981; Bergant & Simpson 1999; Guinot 2001). During this investigation, Equation (11) formulated by Martin *et al.* (1976) was used to study the fluid transients considering a water–air mixture:

$$c_m = \sqrt{\frac{1}{\rho(1-\alpha)((\mu D/Ee) + (\alpha/K_a) + ((1-\alpha)/K_w))}} \tag{11}$$

where K_a is the bulk modulus of elasticity of air, α is the air-void fraction and μ is the pipe constraint factor.

Moreover, if the losses at the junction $(i+1,1)$ are neglected, then:

$$H_{U_{i,n+1}} = H_{U_{i+1,1}} \tag{12}$$

Substituting Equations (3)–(5) and (12) into Equation (2) and eliminating the unknown variables $V_{U_{i,n+1}}$,$Q_{U_{i+1,1}}$, $Q_{U_{i,n+1}}$,

$H_{U_{i+1,1}}$, yields:

$$(H_{U_{i,n+1}} + H_b - z)\left[C_{air} + \frac{\Delta t}{2}(B_{c_i} + B_{c_{i+1}})H_{U_{i,n+1}}\right]^{\kappa} = C \tag{13}$$

$$C_{air} = V_i + \frac{\Delta t}{2}(Q_{i+1,1} - Q_{i,n+1} + C_{(-)} - C_{(+)}) \tag{14}$$

Equation (13) is resolved for $H_{U_{i,n+1}}$ with the method of Newton–Raphson. The values of the other unknown variables can be evaluated from Equations (2) through (12).

For the convergence and stability of the finite difference scheme, the Courant condition always satisfied overall the pressure transient simulations.

$$\frac{\Delta x}{\Delta t} \geq c \tag{15}$$

$$\frac{\Delta x}{\Delta t} \geq c_m \tag{16}$$

During the simulation Δt is fixed, likewise c and c_m should be known and then the numerical model automatically adjusts the value of Δx for each pipeline section.

In this particular investigation, the boundary condition at the upstream end is a constant head tank and at the downstream end a butterfly valve that closes suddenly (closure time 0.15 s). The characteristic equations that define these boundaries are discussed in detail in the standard literature on fluid transients, for instance, Wylie *et al.* (1993) and Chaudhry (2014).

At this stage, it is important to emphasize that the analysis of transients in two-component flows is more complex and difficult than in single-component flows. Further, the probability of occurrence of shock waves due to the steepening of compression waves usually limits the use of the MOC, since it would be necessary to include the shock equations as internal boundary conditions in the characteristic grid (Chaudhry *et al.* 1990). Therefore, the one-dimensional homogeneous model is used to investigate the pressure surges considering two-phase bubbly water–air mixtures downstream of the stationary air pockets. The continuity equations for the gas phase and liquid phase, as well as the dynamic equation for the water–air mixture, yield a system of partial differential equations that will be solved by the explicit–implicit scheme proposed by McGuire & Morris (1975). It is important to highlight that the latter method is used for the computations at the interior grid points.

In the same way, a comparison made by Padmanabhan *et al.* (1978) shows that the explicit–implicit scheme is preferred over the well-known Lax–Wendroff two-step scheme (Lax & Wendroff 1960), since shock wave propagation as well as shock reflections and interactions are better simulated. Further, the explicit–implicit scheme requires about 10% less of the computing time needed by the Lax–Wendroff method.

For the homogeneous model, the water–air bubbly flow is considered as a single pseudofluid with average properties. The relative velocity between the components is neglected in the development of the continuity equations for each phase, and for the dynamic equations for the mixture (Martin *et al.* 1976; Wiggert & Sundquist 1979). Likewise, the system of equations takes into account the compressibility of air and water, as well as the pipe wall elasticity.

Regarding the homogenous model, the following considerations were made. (a) The water–air mixture is a homogenous two-component bubbly flow. Although the growing bubbles may join, for the most part they remain uniformly distributed in a continuous liquid phase along the pipe. (b) The momentum interchange between the air and water components is neglected. (c) The momentum of the air component relative to the liquid is small and hence can be neglected. (d) The average cross-sectional representation of air void fraction, water–air mixture velocity, and component densities can be employed. (e) No gas release and absorption takes place during the transients. (f) The circulation region, also called net air transport, does not extend beyond the end of downward sloping pipe section (see Figure 1).

By using a control-volume approach the conservation of mass can be developed for each phase (Yadigaroglu & Lahey 1976). This formulation is not strictly speaking a separated flow model because it is considered that the relative velocity between the fluids is zero. Therefore, the conservation of mass equation is given by:

$$\frac{\partial}{\partial t}(\rho_a \alpha A) + \frac{\partial}{\partial x}(\rho_a \alpha A v_a) = 0 \tag{17}$$

where ρ_a is air density (kg/m^3), A pipe cross-sectional area (m^2), v_a average air velocity (m/s), t time (s), x axial distance along the pipe (m).

For the liquid phase the conservation of mass equation is written as:

$$\frac{\partial}{\partial t}(\rho(1-\alpha)A)+\frac{\partial}{\partial x}(\rho(1-\alpha)Av)=0 \tag{18}$$

where v is the water velocity in the pipe (m/s), which has been assumed equal to the gas phase velocity.

Neglecting the contribution of the gas phase, the dynamic equation for the water–air mixture can be formulated from a control-volume as:

$$\frac{\partial}{\partial t}[\rho(1-\alpha)Av_m]+\frac{\partial}{\partial x}\left[\rho(1-\alpha)Av_m^2\right]+A\frac{\partial p}{\partial x} + \pi D\tau_0-g\rho(1-\alpha)Asin\theta=0 \tag{19}$$

where p is the average pressure at the particular cross-section (kg/m^2), $v_m=v_a=v$ mixture velocity (m/s), τ_o boundary shear stress (kg/m^2), θ angle of pipe with respect to the horizontal.

The boundary shear stress is based on the definition of the Darcy–Weisbach resistance coefficient f:

$$\tau_0=\frac{f}{8}(1-\alpha)\rho v_m|v_m| \tag{20}$$

The mixture density is:

$$\rho_m=(1-\alpha)\rho+\alpha\rho_a \tag{21}$$

For most of the gas–liquid mixtures, Equation (21) can be approximated by:

$$\rho_m=(1-\alpha)\rho \tag{22}$$

In the numerical model the air-void fraction is calculated with Equation (23), defined as the ratio of the area of the gas phase and the total area in the given cross-section. It is worth noting that for this particular investigation the values of α are considered to remain constant, since it is taken into account that no gas release and absorption occurs during the transients:

$$\alpha=\frac{\beta}{1+\beta} \tag{23}$$

β is the air to water flow ratio:

$$\beta=\frac{Q_a}{Q_w} \tag{24}$$

where Q_a is the air discharge and Q_w the water discharge.

The values of β are calculated using the relationship proposed by Ahmed *et al.* (1984) (Equation (25)). This relationship is used in the numerical model implemented to simulate the two-component fluid transients within the continuous liquid phase downstream of the hydraulic jump, because it is supported on a three-year testing program. A total of 2,250 test runs had been made in closed conduits sloping from horizontal to vertical. Further, the relationship includes the scale effects arising during the air entrainment process:

$$\beta=0.04(F_1-1)^{0.85} \tag{25}$$

where F_1 is the Froude number at the toe of the hydraulic jump.

Equations (17)–(19) can be formulated in conservation form for use by the implicit–explicit scheme. For subsequent development it is convenient to define the total differential operator:

$$\frac{d}{dt}=\frac{\partial}{\partial t}+v\frac{\partial}{\partial x} \tag{26}$$

and the transformations:

$$\frac{1}{\rho_k}\frac{d\rho_k}{dt}=\frac{1}{K_k}\frac{dp}{dt} \tag{27}$$

$$\frac{1}{A}\frac{dA}{dt}=\frac{\mu d}{Ee}\frac{dp}{dt} \tag{28}$$

Substitution of Equations (26)–(28) into Equations (17)–(19) and assuming no gas production results in:

$$\left(\frac{1}{K_a}+\frac{\mu D}{Ee}\right)\frac{dp}{dt}+\frac{1}{\alpha}\frac{d\alpha}{dt}+\frac{\partial v}{\partial x}=0 \tag{29}$$

$$\left(\frac{1}{K_w}+\frac{\mu D}{Ee}\right)\frac{dp}{dt}+\frac{1}{(1-\alpha)}\frac{d(1-\alpha)}{dt}+\frac{\partial v}{\partial x}=0 \tag{30}$$

The simplified dynamic equation for the water–air mixture is given by:

$$\frac{dv}{dt}+\frac{1}{\rho_w(1-\alpha)}\frac{dp}{dx}+\frac{f}{2D}v|v|-gsen\theta=0 \tag{31}$$

The three-equation set represented by Equations (29)–(31) constitute a quasi-linear hyperbolic system that can be rewritten as:

$$\frac{\partial\alpha}{\partial t}+v\frac{\partial\alpha}{\partial x}-\varphi_1\frac{\partial v}{\partial x}=0 \tag{32}$$

$$\frac{\partial p}{\partial t}+v\frac{\partial p}{\partial x}-\varphi_2\left(\frac{\partial\alpha}{\partial t}+v\frac{\partial\alpha}{\partial x}\right)=0 \tag{33}$$

$$\frac{\partial v}{\partial t}+v\frac{\partial v}{\partial x}+\varphi_3\frac{\partial p}{\partial x}=\epsilon_1 \tag{34}$$

where

$$\varphi_1=\alpha(1-\alpha)\left(\frac{1}{K_a}-\frac{1}{K_w}\right)\left[\frac{D\mu}{Ee}+\frac{\alpha}{K_a}+\frac{(1-\alpha)}{K_w}\right]^{-1} \tag{35}$$

$$\varphi_2=\left[\alpha(1-\alpha)\left(\frac{1}{K_a}-\frac{1}{K_w}\right)\right]^{-1} \tag{36}$$

$$\varphi_3=\frac{1}{\rho_w(1-\alpha)} \tag{37}$$

$$\epsilon_1=gsin\theta-\frac{f}{2D}v_m|v_m| \tag{38}$$

To apply the explicit–implicit scheme the set of conservation Equations (32)–(34) is considered to be of the form:

$$\frac{\partial Q_{i1}}{\partial t}+\frac{\partial Q_{i2}}{\partial x}=Q_{i3} \tag{39}$$

where the quantity Q_{i1} (for $i=1, 2, 3$) defines the functions of the pressure, velocity, and void fraction.

The explicit–implicit method conjugates the explicit scheme with the implicit scheme previously formulated by McGuire & Morris (1973) and McGuire & Morris (1974). In the explicit scheme, the three-equation set represented by Equation (39) is approximated by difference formulas, then Q^*_{i1} and Q_{i1} can be found by solving Equations (40) and (41):

$$\begin{aligned}&Q^*_{i1}[(j\Delta x,(m+a)\Delta t)]\\&=\frac{1}{2}\left[Q_{i1}\left\{\left(j+\frac{1}{2}\right)\Delta x,\ m\Delta t\right\}+Q_{i1}\left\{\left(j-\frac{1}{2}\Delta x, m\Delta t\right)\right\}\right]\\&\quad-ar\left[Q_{i2}\left\{\left(j+\frac{1}{2}\right)\Delta x, m\Delta t\right\}-Q_{i2}\left\{\left(j-\frac{1}{2}\right)\Delta x, m\Delta t\right\}\right]\\&\quad+\frac{a\Delta t}{2}\left[Q_{i3}\left\{\left(j+\frac{1}{2}\right)\Delta x, m\Delta t\right\}+Q_{i3}\left\{\left(j-\frac{1}{2}\right)\Delta x, m\Delta t\right\}\right]\end{aligned} \tag{40}$$

$$\begin{aligned}&Q_{i1}[(j\Delta x,(m+1)\Delta t)]=Q_{i1}[j\Delta x,\ m\Delta t]\\&\quad-\frac{r}{2}\left(1-\frac{1}{2a}\right)[Q_{i2}\{(j+1)\Delta x, m\Delta t\}-Q_{i2}\{(j-1)\Delta x, m\Delta t\}]\\&\quad+\frac{r}{2a}\left[Q^*_{i2}\left\{\left(j+\frac{1}{2}\right)\Delta x,(m+a)\Delta t\right\}\right.\\&\quad\left.-Q^*_{i2}\left\{\left(j-\frac{1}{2}\right)\Delta x,(m+a)\Delta t\right\}\right]\\&\quad+\frac{\Delta t}{2}[Q_{i3}\{(j+1)\Delta x, m\Delta t\}+Q_{i3}\{(j-1)\Delta x, m\Delta t\}]\end{aligned} \tag{41}$$

where $(j\Delta x,\ m\Delta t)$ denote the grid points, j and m assume integer values 1, 2, 3, … etc. Δx and Δt refer to the reach length and the computational time step, respectively. The stability of the explicit–implicit scheme is satisfied if and only if $r|\omega|\le 1$ and $-\frac{1}{2}\le ad\le\frac{1}{2}$, where $|\omega|$ is the maximum modulus eigenvalue of the coefficient matrix of the linearized version of the system (Equation (39)). For the implementation of the numerical model the parameters $a=2$ and $d=1/4$ were used for all pressure transient simulations.

In Equations (40) and (41), Q^* denotes the predicted value to Q. The implicit method formulated by McGuire & Morris (1974) consists of Equation (40) and a finite difference approximation for $Q_{i1}[(j\Delta x, (m+1)\Delta t)]$, as follows:

$$\begin{aligned} Q_{i1}[(j\Delta x, (m+1)\Delta t)] &= Q_{i1}[j\Delta x,\ m\Delta t] - \frac{r}{2}\left(\frac{1}{2} + d(a-1)\right) \\ &[Q_{i2}\{(j+1)\Delta x, m\Delta t\} - Q_{i2}\{(j-1)\Delta x, m\Delta t\}] + \frac{r}{2}\left(\frac{1}{2} - ad\right) \\ &[Q_{i2}\{(j+1)\Delta x, (m+1)\Delta t\} - Q_{i2}\{(j-1)\Delta x, (m+1)\Delta t\}] \\ &+ rd\left[Q^*_{i2}\left\{\left(j+\frac{1}{2}\right)\Delta x, (m+a)\Delta t\right\}\right. \\ &\left. -Q^*_{i2}\left\{\left(j-\frac{1}{2}\right)\Delta x, (m+a)\Delta t\right\}\right] \\ &+ \frac{\Delta t}{2}[Q_{i3}\{(j+1)\Delta x, m\Delta t\} + Q_{i3}\{(j-1)\Delta x, m\Delta t\}] \end{aligned} \quad (42)$$

To verify the proposed numerical model, an experimental apparatus made of polyvinyl chloride (PVC) was used to perform hydraulic transient experiments. The setup has a test section that simulates a high point of a pipeline with an undulating profile. During the experiments, the pressure transients were generated by the sudden closure of a butterfly valve with double acting pneumatic actuator located at the downstream end of the test section.

EXPERIMENTAL INVESTIGATION

A setup was implemented in order to study the combined effects on surge pressures of entrapped air pockets ending with a hydraulic jump that seal a conduit with supercritical slope and a homogeneous water–air mixture within the continuous liquid phase immediately downstream of the pockets.

Description of the experimental apparatus

A hydropneumatic vertical standing tank with a capacity of 2.3 m^3 serves as upstream constant head tank. The test section of the setup was 12.6 m in length, and the transparent PVC pipes used have an internal diameter of 200 mm, thus making surface tension effects negligible (Pothof & Clemens 2010, 2011; Pothof 2011). The test section was fixed and mounted on metallic frames. It is formed by an upstream pipe of 4.5 m long and by another downstream pipe section of 7.5 m in length. A plastic hose with a length of 60 cm and an internal diameter of 200 mm was used to connect both transparent PVC pipe sections. At the end of the test section, a gooseneck pipe was connected by which the water returned to the rectangular tank. A schematic drawing of the experimental apparatus is shown in Figure 2.

Instrumentation of the experimental apparatus

The following measurement instruments were used in the experimental investigation.

One-quarter turn ball valves were placed at every 15 cm throughout the test section (tapping points) allowing air to enter and to exhaust during dewatering and filling operations. In addition, a compressor was used to inject air to the pipe through a tapping point.

The water depths underneath the air pockets immediately upstream of the hydraulic jump were measured in two ways. (1) An acoustic metallic sensor was introduced through the tapping points, once the point of the sensor was in contact with the water surface, the electronic sound system emitted a whistle, and then the measurement was taken. (2) When the beginning of jumps did not coincide with the location of a tapping point, the depths were measured circumferentially from outside of the pipe and corrected for pipe wall thickness.

A U-tube manometer filled with water served to measure the total head losses (i.e., pipe friction, pipe entry, bends, energy loss in the jump, and butterfly valve) throughout the transparent pipe section with and without air pockets. The difference in elevation Δh read directly from the manometer was utilized to compute the friction factor f_{exp} by the well-known formula of Darcy–Weisbach.

The initial steady-state water flow rate in the experimental apparatus was measured with an ultrasonic flowmeter PrimeFlo-T, Model RXG 845.

A butterfly valve with double acting pneumatic actuator was installed at the downstream end of the test section to cause the transients. Two piezoelectric transducers (Omegadyne, Model PX103U1) were used for the pressure measurements in the test section. They were placed at 4.0 m and 5.4 m downstream from the hydropneumatic tank, respectively. The transducers are capable of measuring

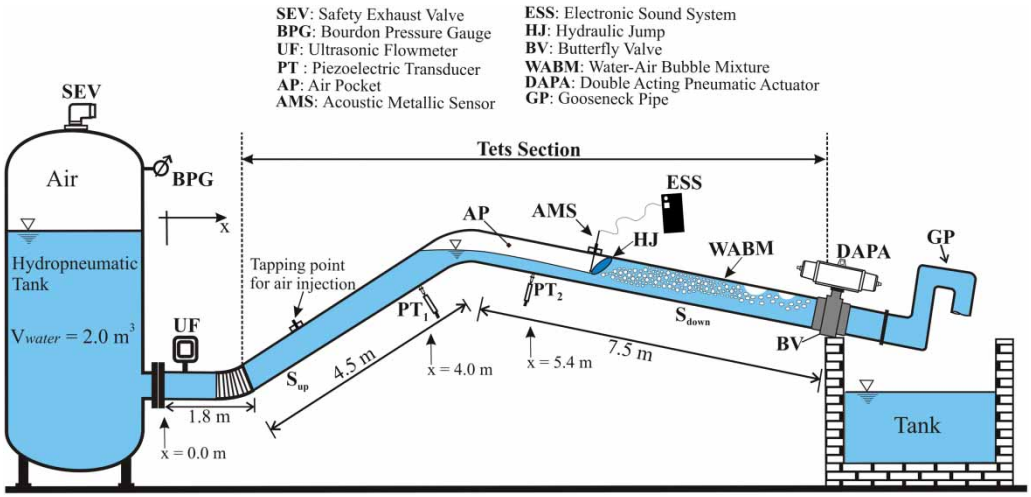

Figure 2 | Experimental apparatus.

pressures in the range of 0 to 690 kPa with an accuracy of ±0.5%. The signal of the sensors was registered by means of a demodulator (Validyne, Model CD23) and a data acquisition board (National Instruments PCI-6281). The pressure surge data of the two sensors were stored in the hard disk of a laptop for analysis. In addition, a pre-triggering program was implemented to register the air pocket pressure with the transducers at steady state before energizing the double acting pneumatic actuator.

Experimental procedure

In order to investigate the effect on pressure surges of air pockets with a water–air bubble mixture downstream of them, two different experiments were developed in the setup. Subsequently, experimental data obtained during the measurements were utilized to simulate numerically the hydraulic transients with and without entrapped air. For both experiments, each run was repeated at least five times to avoid errors. For all tests, pressure transient oscillations showed repetitiveness and the same pressure pattern.

The absolute head at the upstream tank was constant throughout the experiments, equal to 139.7 kPa (20 psi). Three different initial air pocket volumes were tested, for each of the four water flow rates that ranged from 0.020 m^3/s to 0.035 m^3/s.

A hydropneumatic vertical standing tank with a capacity of 2.3 m^3 serves as upstream constant head tank. The tank is equipped with a safety exhaust valve at its top, a Bourdon pressure gauge to register the pressure during the test runs, and sight plastic to visualize water level in the tank. Minimum air volumes of 0.3 m^3 and 2.0 m^3 of water were maintained in the tank to ensure that it serves as a reservoir. In addition, the pressure in the tank did not register any variation during the fast transient (just a few seconds).

The upstream portion of the test section has an adverse slope of $S_{up} = -0.532$ ($\theta = -28°$), and the downward sloping pipe was set at $S_{down} = 0.466$ ($\theta = 25°$) to simulate a high point of a pipeline with an undulating profile. During the tests, stationary air pockets accumulated along the control section located at the transition between pipes with sub- and supercritical slope (S_{up} and S_{down}), always ending in a hydraulic jump at the downward sloping pipe. The turbulence kinetic energy of the jump generated small air bubbles that were entrained and transported along the pipe producing a two-component bubbly flow within the continuous liquid phase (see Figure 2).

As previously mentioned, it is well-known that small air pockets can amplify pressure surges great enough to produce pipe rupture. Further, plastic pipes are significantly limited due to the low range of stress values that this kind of material can support. Therefore, enough air was injected at each run to produce the accumulation of large stationary air pockets at the test section of the setup to avoid the rupture of the PVC pipes.

Experiment 1. The test section was flowing full without air. The pressure transients were generated closing the butterfly valve by the pneumatic actuator from full opening in 0.15 s and assuming a linear valve closure.

Experiment 2. In order to investigate the effect on hydraulic transients of entrapped air after the sudden closure (0.15 s considering a linear closing valve law) of the butterfly valve that was fully open, the following procedure was performed: the test section was flowing full, while air was injected through a tapping point located at the beginning of the upward sloping pipe of the apparatus. The ball valve was open to allow injection of air by means of a flexible tubing connected to a compressor. The air was transported by the water flow along the pipe to the high point at the change of slope, where air accumulated in the form of an air pocket that remained stationary. The hydraulic jump that filled the conduit at the downward pipe with supercritical slope was forced by locating a gooseneck pipe downstream of the butterfly valve. Following the jump the regime presented was the bubbly flow.

During the investigation, preliminary runs were developed based on the studies carried out by Kalinske & Robertson (1943) and Kalinske & Bliss (1943), in order to analyze the behavior of the air bubbles distributed within the continuous liquid phase downstream of the jumps. Experimental observations confirmed that water flow rates ranging from 0.020 m^3/s to 0.035 m^3/s are insufficient to remove the small bubbles from the downward sloping pipe, likewise the bubbles would gradually coalesce into large bubbles and eventually move in the upstream direction through the jump towards the air pocket. Accordingly, it was considered that the volume of air remained invariant at each run.

In addition, the water depths at the point of hydraulic jump initiation were recorded to estimate the air entrained by the hydraulic jump β and the void fraction α in the water–air mixture.

Once the test was finished, the air was released from the test section and the steps repeated at a different injected air volume.

During experiment 2, the air pocket volume decreased in size because the pressure in the transparent pipe section is higher than the atmospheric pressure in Mexico City (≈78.5 kPa) and therefore its volume could not be measured prior to injection. In order to compute the air pockets' volumes at the test section, the relationship (Equation (43)) proposed by Pozos *et al.* (2010) was used.

$$V_{AirPocket} = A_{up}L_{up} + A_{down}L_{down} \tag{43}$$

where $V_{\mathrm{AirPocket}}$ is the air pocket volume, A_{up} and A_{down} are the areas of the air pocket at the upward and downward pipes of the test section, respectively. L_{up} and L_{down} denote the lengths of the air pocket at the upstream and downstream pipe portions of the test section, respectively.

Table 1 states the air pocket volumes calculated using Equation (43), the length of the flow profiles underneath the air pockets, water flow discharges, the absolute pressure inside the pocket at steady-state, as well as the air-void fractions. In addition, the water depths 'y' at the point of hydraulic jump initiation and the air–water flow ratio β are summarized.

RESULTS AND DISCUSSION

Results from the experimental investigation and simulations in numerical model are presented in this section. Figure 3 shows the pressure transient comparison of the experimental results and the pressure transient simulations following the closure of the butterfly valve without any air in the test section by using only the MOC due to no air being entrapped at the high point. It can be observed that the pressure amplitudes calculated are slightly higher than the measured values. This could be due to uncertainty in the measurements. Therefore, it can be stated that the numerical and experimental results have a good agreement.

Figures 4–6 show the effect of three different air pocket volumes on pressure transients for a water discharge of 0.02 m^3/s (20 L/s). It can be observed that the presence of air in the test section clearly reduce the amplitude of the pressure oscillations, and also increase the period of the waves. It is important to emphasize that the pressures obtained from the piezoelectric transducers' measurements gave similar results. Further, pressure transient simulations with and without air and different water flow discharges showed the same pressure pattern. Therefore, only part of the results are presented.

Table 1 | Air pocket volumes and lengths of flow profiles

Volume of air (m^3) Equation (43)	Length of the air pocket profiles (m) Profile upstream	Length of the air pocket profiles (m) Profile downstream	Absolute pressure in the air pocket (kPa)	Water depth y(m)	β (–)	α (%)
$Q_w = 0.02$ (m^3/s)						
0.0331	0.564	0.503	138.7	0.043	0.106	9.6
0.0387	0.564	0.682	139.2	0.039	0.124	11.1
0.0468	0.564	0.942	139.9	0.036	0.147	12.8
$Q_w = 0.025$ (m^3/s)						
0.0306	0.441	0.574	139.1	0.048	0.106	9.7
0.0368	0.441	0.778	139.8	0.044	0.125	11.1
0.0460	0.441	1.072	140.2	0.041	0.148	12.9
$Q_w = 0.03$ (m^3/s)						
0.0360	0.294	0.868	139.7	0.049	0.126	11.2
0.0462	0.294	1.196	140.1	0.045	0.148	12.9
0.0616	0.294	1.694	140.9	0.041	0.177	15.0
$Q_w = 0.035$ (m^3/s)						
0.0285	0.209	0.711	139.3	0.058	0.109	9.8
0.0362	0.209	0.962	139.3	0.054	0.127	11.3
0.0474	0.209	1.324	140.7	0.049	0.150	13.1

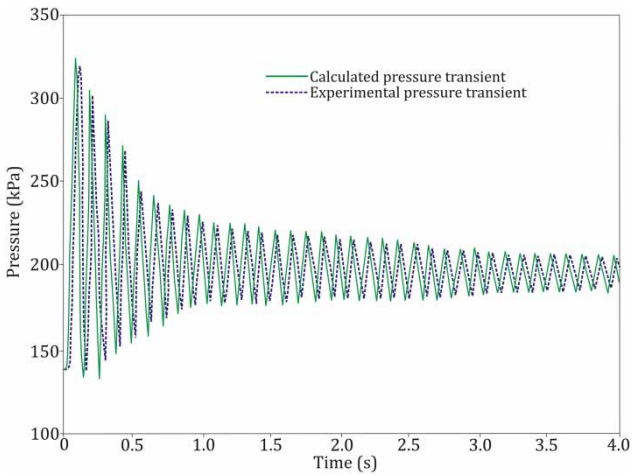

Figure 3 | Pressure transient comparison between experimental and computed results without air.

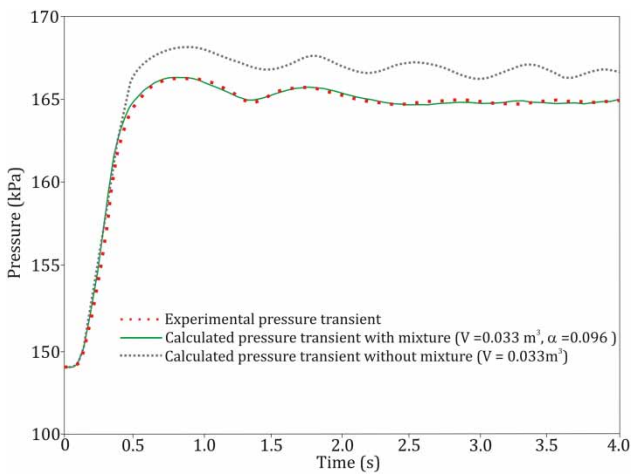

Figure 4 | Pressure transient comparison between experimental and computed results with air.

Figure 4 shows the numerical comparison of the calculated results from the simulations of fluid transients with an air pocket ($V = 0.033\ m^3$) with and without a water–air mixture (air-void fraction, $\alpha = 0.096$) immediately downstream of it, as well as the pressure transient registered during the experiment. From the results obtained and depicted, it is noticeable that the air pocket volume has an important dampening effect. Moreover, it can be seen that when a water–air mixture occurs downstream of the air pocket, the reduction of the pressure transient envelope is even more considerable than that compared without water–air mixture.

From the results presented in Figures 5 and 6 it is demonstrated that the distribution of the air void fraction greatly influences the pressure transients. It can be observed that the pressure oscillations decrease considerably throughout the test section with increasing the air-void fraction α and the air-pocket volume V.

From the computations obtained, it can be seen in Figure 6 that the reflection of the transient pressure wave almost disappears due to the presence of the mixture of air and water. For this specific situation this volume of air with its corresponding air-void fraction ($V = 0.047$ m^3, $\alpha = 0.128$) has a beneficial effect.

For experiment 2, each run was repeated five times to determine the consistency of results. In all cases, pressure transient oscillations show the repetitiveness of the transient. For example, in Figure 7 the pressure surges obtained from the piezoelectric transducer 2 (PT_2) following the closure of the butterfly valve is plotted for the simulations of fluid transients with a water discharge of $Q_w = 0.02$ m^3/s, an air pocket volume of V = 0.033 m^3, and an air-void fraction of $\alpha = 0.096$. Data for all the five runs exhibit the same pressure pattern and small deviations.

From the previous graphs, it is possible to suggest that the large air pockets with a water–air mixture downstream of them contribute to reduce considerably the pressure transients in the test section of the experimental apparatus. Further, it can be stated that the cushioning effect produced by the large air volumes and the corresponding air void fractions on the transients is even more considerable than that compared without bubbly flow air content.

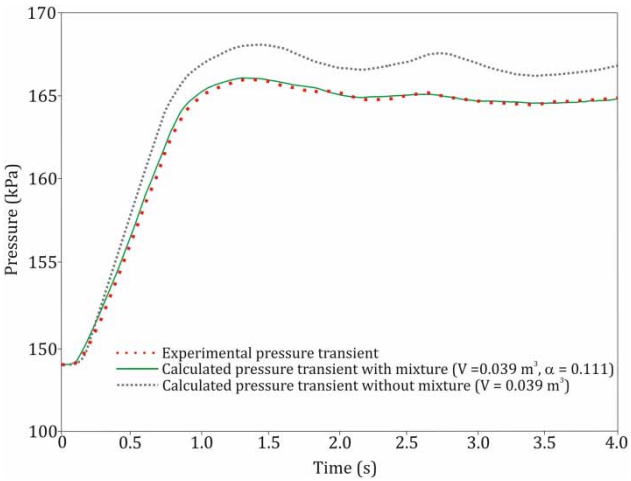

Figure 5 | Pressure transient comparison between experimental and computed results with air.

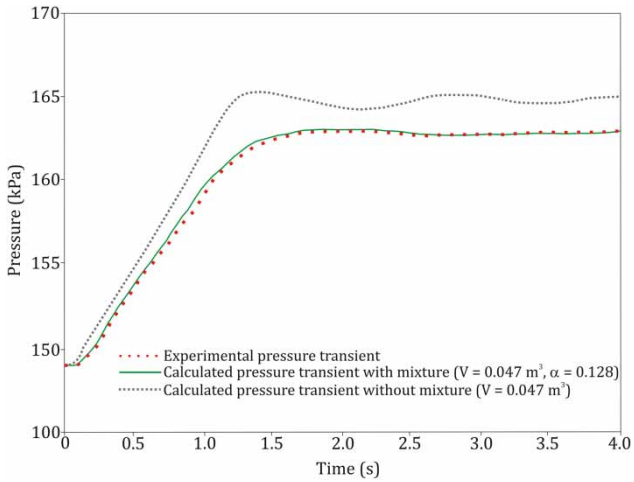

Figure 6 | Pressure transient comparison between experimental and computed results with air.

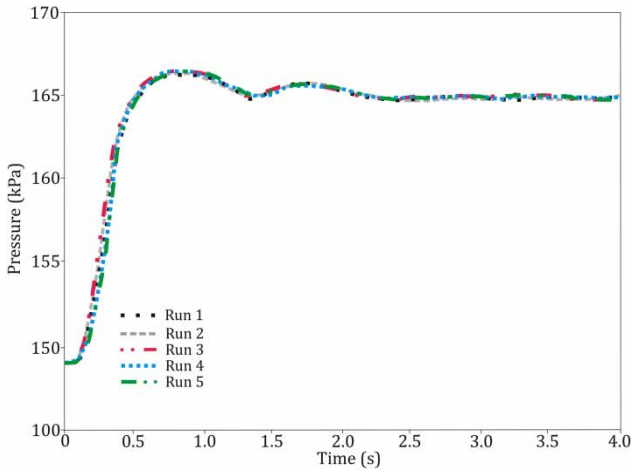

Figure 7 | Pressure transients for all runs with $Q_w = 0.02$ m^3/s, V = 0.033 m^3, and $\alpha = 0.096$.

The important dampening effect on the experimental and calculated pressure transients might be explained as follows, when the air-pocket volume increases the water depth at the point of hydraulic initiation decreases (see Table 1), increasing the intensity of turbulence in the hydraulic jump, which entrains more small air bubbles from the air pocket, reducing the wave celerity passing through the water–air mixture (Pearsall 1965; Davis 1980; Ewing 1980).

It must be highlighted that the measurements of pressure transients compares favorably with the calculated

pressure transients considering the air-pocket volume and its corresponding air-void fraction.

CONCLUSIONS

Air pockets can accumulate at high points of pipelines with undulating profile, and at the end of the air pockets a hydraulic jump usually occurs. The turbulence action at the jump generates small air bubbles that are entrained and transported along the pipe producing a two-component bubbly flow within the continuous liquid phase. A numerical model is developed here to simulate the combined effect on pressure transients of air pockets and homogenous water–air bubble mixtures. The proposed model is validated by using an experimental apparatus to perform hydraulic transient experiments.

The numerical model is based on the explicit–implicit scheme proposed by McGuire & Morris (1975) and the MOC for solving the quasi-linear hyperbolic partial differential equations for transient two-phase flow expressed in conservation form, and the air pocket polytropic equation, respectively. The explicit–implicit method is preferred over the Lax–Wendroff method and the MOC, because it possesses the facility to reduce the overshooting and attendant high-frequency oscillations by selecting the most adequate values of two parameters (a and d) used during the simulations. Further, the shock-waves as well as the shock reflections are simulated better, and the computation time is reduced.

Pressure transients resulting from the rapid closure of the downstream valve in a test section of irregular profile containing an air pocket and a water–air mixture can be reasonably well predicted by the numerical model herein presented.

The results show that the large air pockets with a water–air mixture downstream of them contribute to diminish significantly the pressure transients in the test section of the experimental apparatus. Moreover, it can be stated that the dampening effect generated by the large air pocket volumes and the corresponding air-void fractions on the transients is even more considerable than that compared without bubbly flow air content, acting as effective accumulators, suppressing the pressure transients.

The important cushioning effect on the experimental and simulated pressure transients might be explained as follows, when the air-pocket volume increases the water depth at the point of hydraulic initiation decreases, causing an increment in the intensity of turbulence in the hydraulic jump, which entrains more small air bubbles from the air pocket, reducing the wave celerity passing through the water–air mixture.

In terms of future research, both experimental and analytical studies are required for scenarios with small air-pocket volumes to analyze the possible occurrence of gas release and absorption during the transients. It is recommended to perform the experimental investigation in an apparatus with a test section made of metallic pipes, since plastic pipes are significantly limited due to the low range of stress values that this kind of material can support.

ACKNOWLEDGEMENTS

The author is grateful for the financial support from the Dirección General de Asuntos del Personal Académico (DGAPA-UNAM) (Proyecto PAPIIT IA100213-2).

REFERENCES

Ahmed, A. A., Ervine, D. A. & McKeogh, E. J. 1984 The process of aeration in closed conduit hydraulic structures. In: *Proceedings of a Symposium on Scale Effects in Modelling Hydraulic Structures (*H. Kobus, ed.). Technische Akademie Esslingen, Germany, 3–6 September, pp. 1–11.

Almeida, A. B. & Ramos, H. M. 2010 Water supply operation: diagnosis and reliability analysis in a Lisbon pumping system. *Journal of Water Supply: Research and Technology-Aqua* **59** (1), 66–78.

Apollonio, C., Balacco, G., Fontana, N., Giugni, M., Marini, G. & Piccinni, A. F. 2016 Hydraulic transients caused by air expulsion during rapid filling of undulating pipelines. *Water* **8**, 1–12.

Arregui, F., Garcia, J., Kruisbrink, A., Cabrera, E., Fuertes, V. S., Palau, C. V. & Gascón, L. 2003 Air valves dynamic behaviour. In: *Proceedings of the PEDS 2003 – Pumps, Electromechanical Devices and Systems Applied to Urban Water Management*, 22–25 April, Valencia, Spain.

Balacco, G., Apollonio, C. & Piccinni, A. F. 2015 Experimental analysis of air valve behaviour during hydraulic transients. *Journal of Applied Water Engineering and Research* **3** (1), 3–11.

Bergant, A. & Simpson, A. R. 1999 Pipeline column separation flow regimes. *Journal of Hydraulic Engineering* **125** (8), 835–848.

Besharat, M., Tarinejad, R. & Ramos, H. M. 2016 The effect of water hammer on a confined air pocket towards flow energy storage system. *Journal of Water Supply: Research and Technology-Aqua* **65** (2), 116–126.

Burrows, R. 2003 A cautionary note on the operation of pumping mains without appropriate surge control and the potentially detrimental impact of small air pockets. In: *Proceedings of the IWA International Conference*, 22–25 April, Valencia, Spain.

Burrows, R. & Qiu, D. Q. 1995 Effect of air pockets on pipeline surge pressure. *Proceedings of the Institute of Civil Engineers – Water Maritime and Energy* **112** (4), 349–361.

Carlos, M., Arregui, F. G., Cabrera, E. & Palau, V. 2011 Understanding air release through air valves. *Journal of Hydraulic Engineering* **137** (4), 461–469.

Chaudhry, M. H. 2014 *Applied Hydraulic Transients,* 3rd edn. Springer, New York.

Chaudhry, M. H., Bhallamudi, S. M., Martin, C. S. & Naghash, M. 1990 Analysis of transient pressures in bubbly, homogeneous, gas-liquid mixtures. *Journal of Fluids Engineering* **112**, 225–231.

Davis, M. R. 1980 Structure and analysis of gas-liquid mixture flow. In: *7th Australasian Conference on Hydraulics and Fluid Mechanics*, Institution of Engineers, 18–22 August, Brisbane, Australia, pp. 416–419.

De Martino, G., Giugni, M., Viparelli, M. & Gisonni, C. 2000 Pressure surges in water mains caused by air release. In: *Proceedings of the 8th International Conference on Pressure Surges – Safe Design and Operation of Industrial Pipe Systems*, 12–14 April, The Hague, The Netherlands, pp. 147–159.

Edmunds, R. C. 1979 Air binding in pipes. *Journal of the American Water Works Association* **71**, 272–277.

Ewing, D. J. F. 1980 Allowing for free air in waterhammer analysis. In: *Proceedings of the 3rd International Conference on Pressure Surge*, 25–27 March, BHRA, Canterbury, UK, pp. 127–146.

Falvey, H. T. 1980 *Air-Water Flow in Hydraulic Systems, Engineering Monograph No. 41*. Bureau of Reclamation, Denver, CO.

Fanelli, M. & Reali, M. 1975 A theoretical determination of the celerity of water hammer waves in a two-phase fluid mixture. *L'Energia Elettrica* **4**, 183–485.

Fox, J. A. 1977 *Hydraulic Analysis of Unsteady Flow in Pipe Networks*. MacMillan Press, London, UK.

Fuertes, V. S., Arregui, F., Cabrera, E. & Iglesias, P. L. 2000 Experimental setup for entrapped air pockets model validation. In: *Proceedings of the 8th International Conference on Pressure Surges – Safe Design and Operation of Industrial Pipe Systems*, 12–14 April, The Hague, The Netherlands, Vol. 39, pp. 133–146.

Gahan, C. M. 2004 *A Review of the Problem of Air Release/ Collection in Water Pipelines with in-Depth Study of the Effects of Entrapped Air on Pressure Transients*. MRes thesis, University of Liverpool, UK.

Guinot, V. 2001 Numerical simulation of two-phase flow in pipes using Godunov method. *International Journal for Numerical Methods in Engineering* **50** (5), 1169–1189.

Ivetic, M. V. 2004 Forensic transient analyses of two pipeline failures. *Urban Water Journal* **1** (2), 85–95.

Izquierdo, J., Fuertes, V. S., Cabrera, E., Iglesias, P. L. & Garcia-Serra, J. 1999 Pipeline start-up with entrapped air. *Journal of Hydraulic Research* **37** (5), 579–590.

Jönsson, L. 1985 Maximum transient pressures in a conduit with check valve and air entrainment. In: *Proceedings of International Conference on the Hydraulics of Pumping Stations*, 17–19 September, BHRA, Manchester, UK, pp. 55–76.

Jönsson, L. 1992 Anomalous pressure transients in sewage lines. In *Proceedings of the International Conference on Unsteady Flow and Transients*, 29 September–1 October, BHRA, Durham, UK, pp. 251–258.

Kalinske, A. A. & Bliss, P. H. 1943 Removal of air from pipelines by flowing water. *Journal of Hydraulic Engineering* **13** (10), 480–482.

Kalinske, A. A. & Robertson, J. M. 1943 Closed conduit flow. *Journal of Hydraulic Engineering* **108**, 1435–1447.

Kalkwijk, J. P. T. & Kranenburg, C. 1971 Cavitation in horizontal pipelines due to water hammer. *Journal of the Hydraulics Division, ASCE* **97**, 1585–1605.

Kobori, T., Yokoyama, S. & Miyashiro, H. 1955 Propagation velocity of pressure wave in pipe line. *Hitachi Hyoron* **37** (10), 1407–1411.

Kruinsbrick, A. C. H., Arregui, F., Carlos, M. & Bergant, A. 2004 Dynamic performance characterization of air valves. In: *Proceedings of the 9th International Conference on Pressure Surges*, 24–26 March, Chester, UK, pp. 33–48.

Lauchlan, C. S., Escarameia, M., May, R. W. P., Burrows, R. & Gahan, C. M. 2005 *Air in Pipelines: A Literature Review. Report SR649*, HR Wallingford, UK.

Lax, P. & Wendroff, B. 1960 Systems of conservation laws. *Communications on Pure and Applied Mathematics* **13** (2), 217–237.

Lee, N. H. 2005 *Effect of Pressurization and Expulsion of Entrapped Air in Pipelines*. PhD thesis, Georgia Institute of Technology, Atlanta, GA, USA.

Lee, N. H. & Martin, C. S. 1999 Experimental and analytical investigation of entrapped air in a horizontal pipe. In: *Proceedings of the 3rd ASME/JSME Joint Fluids Engineering Conference*, 18–23 July, San Francisco, CA, USA.

Leon, A. S. 2006 *Improved Modeling of Unsteady Free Surface, Pressurized and Mixed Flows in Storm-Sewer Systems*. PhD thesis, Department of Civil and Environmental Engineering, University of Illinois at Urbana-Champaign, Urbana, IL, USA.

Leon, A. S., Ghidaoui, M. S., Schmidt, A. R. & Garcia, M. H. 2010 A robust two-equation model for transient-mixed flows. *Journal of Hydraulic Research* **48** (1), 44–56.

Martin, C. S. 1976 Entrapped air in pipelines. In: *Proceedings of the Second International Conference on Pressure Surges*, 22–24 September, London, UK, pp. 15–28.

Martin, C. S. 1996 Two-phase gas-liquid experiences in fluid transients. In: *Proceedings of the 7th International Conference on Pressure Surge and Fluid Transients in Pipelines and Open Channels*, 16–18 April, Harrogate, UK, pp. 65–81.

Martin, C. S. & Lee, N. H. 2000 Rapid expulsion of entrapped air through an orifice. In: *Proceedings of the 8th International Conference on Pressure Surges – Safe Design and Operation of Industrial Pipe Systems*, 12–14 April, The Hague, The Netherlands, pp. 125–132.

Martin, C. S., Padmanabhan, M. & Wiggert, D. C. 1976 Pressure wave propagation in two-phase bubbly air-water mixtures. In: *Proceedings of the 2nd International Conference on Pressure Surges*, 22–24 September, London, UK, pp. 1–16.

Martins, S. C., Ramos, H. M. & Almeida, A. B. 2015 Conceptual analogy for modelling entrapped air action in hydraulic systems. *Journal of Hydraulic Research* **53** (5), 678–686.

McGuire, G. R. & Morris, J. L. 1973 A class of second-order accurate methods for the solution of systems of conservation laws. *Journal of Computational Physics* **11** (4), 531–549.

McGuire, G. R. & Morris, J. L. 1974 A class of implicit, second-order accurate, dissipative schemes for solving systems of conservation laws. *Journal of Computational Physics* **14** (2), 126–147.

McGuire, G. R. & Morris, J. L. 1975 Explicit-implicit schemes for the numerical solution of nonlinear hyperbolic systems. *Mathematics of Computation* **29** (130), 407–424.

Padmanabhan, M., Ames, W. F. & Martin, C. S. 1978 Numerical analysis of pressure transients in bubbly two-phase mixtures by explicit-implicit methods. *Journal of Engineering Mathematics* **12** (1), 83–93.

Pearsall, I. S. 1965 The velocity of water hammer waves. In: *Symposium on Surge in Pipelines*, Institution of Mechanical Engineers, Sage UK, London, Vol. 180, Part 3E, pp. 12–20.

Pothof, I. W. M. 2011 *Co-current Air-Water Flow in Downward Sloping Pipes, Transport of Capacity Reducing Gas Pocket in Wastewater Mains*. PhD thesis, Delft University of Technology, Delft, The Netherlands.

Pothof, I. W. M. & Clemens, F. H. L. R. 2010 On elongated air pockets in downward sloping and inclined pipes. *Journal of Hydraulic Research* **48** (4), 499–503.

Pothof, I. W. M. & Clemens, F. H. L. R. 2011 Experimental study of air–water flow in downward sloping pipes. *International Journal of Multiphase Flow* **37** (3), 278–292.

Pozos, O. 2007 *Investigation on the Effects of Entrained Air in Pipelines*. PhD thesis, University of Stuttgart, Stuttgart, Germany.

Pozos, O., Giesecke, J., Marx, W., Rodal, E. A. & Sanchez, A. 2010 Experimental investigation of air pockets in pumping pipeline systems. *Journal of Hydraulic Research* **48** (2), 269–273.

Pozos-Estrada, O., Fuentes-Mariles, O. A. & Pozos-Estrada, A. 2012 Gas pockets in a wastewater rising main: a case study. *Water Science & Technology* **66** (10), 2265–2274.

Pozos-Estrada, O., Sánchez-Huerta, A., Breña-Naranjo, J. A. & Pedrozo-Acuña, A. 2016 Failure analysis of a water supply pumping pipeline system. *Water* **8** (9), 395.

Qiu, D. Q. 1995 *Transient Analysis and the Effect of Air Pockets in a Pipeline*. PhD thesis, University of Liverpool, Liverpool, UK.

Qiu, D. Q. & Burrows, R. 1996 Prediction of pressure transients with entrapped air in a pipeline. In: *Proceedings of the 7th International Conference on Pressure Surge and Fluid Transients in Pipelines and Open Channels*, 16–18 April, BHRA, Harrogate, UK, pp. 251–263.

Raiteri, E. & Siccardi, F. 1975 Transients in conduits conveying a two phase bubbly flow: experimental measurements of celerity. *L'Energia Elettrica* **5**, 256–261.

Rath, H. J. 1981 Nonlinear propagation of pressure waves in elastic tubes containing bubbly air-water mixtures. In: *Proceedings of the Fifth International Symposium and International Association for Hydraulic Research Working Group Meeting on Water-Column Separation*, Obemach, Universities of Hanover and Munich, Germany, pp. 197–228.

Richards, R. T. 1962 Air binding in water pipelines. *Journal of the American Water Works Association* **54** (6), 719–730.

Sailer, R. E. 1955 San Diego Aqueduct. *Journal of Civil Engineering* **268**, 38–40.

Soares, A. K., Covas, D. I. & Reis, L. F. R. 2011 Leak detection by inverse transient analysis in an experimental PVC pipe system. *Journal of Hydroinformatics* **13** (2), 153–166.

Stephenson, D. 1997 Effects of air valves and pipework on water hammer pressure. *Journal of Transportation Engineering* **123** (2), 101–106.

Sun, J., Wang, R. & Duan, H. F. 2016 Multiple-fault detection in water pipelines using transient-based time-frequency analysis. *Journal of Hydroinformatics* **18** (6), 975–989.

Thomas, S. 2003 *Air Management in Water Distribution Systems: A New Understanding of Air Transfer. Clear Water Legacy,* Burlington, Canada.

Thorley, A. R. D. 2004 *Fluid Transients in Pipeline Systems,* 2nd edn. John Wiley & Sons, London, UK.

Trindade, B. C. & Vasconcelos, J. G. 2013 Modeling of water pipeline filling events accounting for air phase interactions. *Journal of Hydraulic Engineering* **139** (9), 921–934.

Vasconcelos, J. G. 2005 *Dynamic Approach to the Description of Flow Regime Transition in Stormwater Systems*. PhD thesis, Department of Civil and Environmental Engineering, University of Michigan, Ann Arbor, MI, USA.

Vasconcelos, J. G., Klaver, P. R. & Lautenbach, D. J. 2015 Flow regime transition simulation incorporating entrapped air pocket effects. *Urban Water Journal* **12** (6), 488–501.

Walski, T. M., Barnhart, T., Driscoll, J. & Yencha, R. 1994 Hydraulics of corrosive gas pockets in force mains. *Water Environment Research* **66** (6), 772–778.

Wiggert, D. C. & Sundquist, M. J. 1979 The effect of gaseous cavitation on fluid transients. *Journal of Fluids Engineering* **101** (1), 79–86.

Wisner, P. E., Mohsen, F. N. & Kouwen, N. 1975 Removal of air from water lines by hydraulic means. *Journal of the Hydraulics Division* **101** (2), 243–257.

Wright, S. J., Lewis, J. W. & Vasconcelos, J. G. 2011 Physical processes resulting in geysers in rapidly filling storm-water tunnels. *Journal of Irrigation and Drainage Engineering* **137** (3), 199–202.

Wylie, E. B., Streeter, V. L. & Suo, L. 1993 *Fluid Transients in Systems.* Prentice Hall, Englewood Cliffs, NJ, USA.

Yadigaroglu, G. & Lahey Jr, R. T. 1976 On the various forms of the conservation equations in two-phase flow. *International Journal of Multiphase Flow* **2** (5), 477–494.

Zhou, F. 2000 *Effects of Trapped Air on Flow Transients in Rapidly Filling Sewers*. PhD thesis, University of Alberta, Edmonton, Canada.

Zhou, F., Hicks, F. E. & Steffler, P. M. 2002 Transient flow in a rapidly filling horizontal pipe containing trapped air. *Journal of Hydraulic Engineering* **128** (2), 625–634.

Zhou, L., Liu, D. & Karney, B. 2013 Investigation of hydraulic transients of two entrapped air pockets in a water pipeline. *Journal of Hydraulic Engineering* **139** (9), 949–959.

First received 18 January 2017; accepted in revised form 22 November 2017. Available online 12 December 2017